JVST B
Journal of Vacuum Science & Technology B

Reduction of exposing time in massively-parallel E-beam systems

Cite as: J. Vac. Sci. Technol. B **40**, 032602 (2022); https://doi.org/10.1116/6.0001722
Submitted: 26 December 2021 • Accepted: 12 April 2022 • Published Online: 05 May 2022

Md Nabid Hasan, Soo-Young Lee, Byung-Sup Ahn, et al.

JVST B
Journal of Vacuum Science & Technology B

ARTICLE

avs.scitation.org/journal/jvb

Reduction of exposing time in massively-parallel E-beam systems

Cite as: J. Vac. Sci. Technol. B 40, 032602 (2022); doi: 10.1116/6.0001722
Submitted: 26 December 2021 · Accepted: 12 April 2022 ·
Published Online: 5 May 2022

Md Nabid Hasan,[1] Soo-Young Lee,[1,a)] Byung-Sup Ahn,[2] Jin Choi,[2] and Joon-Soo Park[2]

AFFILIATIONS

[1]Department of Electrical and Computer Engineering, Auburn University, Auburn, Alabama 36849
[2]Samsung Electronics, Mask Development Team, 16 Banwol-Dong, Hwasung, Kyunggi-Do 18448, Korea

[a)]leesooy@eng.auburn.edu

ABSTRACT

Several writing methods were previously introduced for massively parallel electron-beam systems, e.g., single-row writing and multirow writing. A straightforward application of these methods for realizing nonuniform dose distributions often required for the proximity effect correction (PEC) including line/space patterns would turn off certain beams, sometimes all, selectively in several cycles. Consequently, the utilization of beams is reduced considerably. In this study, two different approaches to increasing the beam utilization and thereby reducing the exposing (writing) time are investigated, i.e., lowering the dose difference among the regions of a feature while implementing the PEC and utilizing the cycles with all the beams turned off. It has been shown that with these methods, the exposing time can be reduced significantly.

I. INTRODUCTION

The electron-beam (e-beam) lithography is capable of writing complex and fine-feature patterns directly onto a substrate.[1–5] But, the main disadvantage of this maskless lithography technique is low throughput, which limits its application in the fabrication of large-scale photomasks. E-beam lithographic systems with multiple beams were introduced for improving the writing throughput significantly.[6,7] The write time of a mask sized $100 \times 130\,\text{mm}^2$ is 30+ h on a conventional single-beam system while less than 10 h on a massively-parallel e-beam system (MPES).[8] In an MPES, e.g., the eMET,[9] MBM-1000,[10] and MAPPER Lithography FLX-1200 tool,[11] there are a large number of programmable beams, e.g., 512×512, of which optimal utilization is critical to maximizing the efficiency of the system.

Several writing methods have been developed for the MPES. In single-row writing (SRW),[12] a beam or a group of beams exposes pixels from a single row in each writing path, while a beam exposes pixels from multiple rows in each writing path in multirow writing (MRW).[13] In each writing method, when the beams in the system are on throughout the exposing process, a uniform dose distribution is achieved, i.e., the same dose is given to all the pixels within a feature or a pattern. To expose the pixels in a line/space pattern or realize a nonuniform dose distribution often required for proximity effect correction (PEC), certain beams need to be selectively turned off during the exposing process for a uniform dose distribution. The beams to be turned off in each cycle are determined based on the width of the spaces between two features and the shape of target dose distribution. However, these writing methods do not guarantee the shortest exposing time that is achievable on an MPES. This is because certain beams may be turned off in multiple cycles when they fall over the spaces between features in a pattern or when they fall over the pixels requiring lower doses than others. It is possible that all beams in a system are turned off in a cycle, which is referred to as "empty cycle." To improve the utilization of beams and thereby reduce the exposing time, a new writing method may be developed, which can remove the empty cycles during the exposing process. Also, the reduction of exposing time can be attempted when the spatial dose distribution is adjusted for the PEC. If the utilization of beams is not considered, the largest dose difference between any two regions can be significant causing a lot of beams to be turned off in multiple cycles during the exposing process. However, no study has been done on the PEC considering the utilization of beams in an MPES.

In this study, a new writing method is designed to utilize the empty cycles in conventional writing (SRW and MRW) methods while realizing the target dose distribution in a line/space pattern

by adjusting the deflection angle of the beams. The number of empty cycles in the conventional writing methods can vary depending on the widths of feature, space and pattern, the beam interval, the target dose distribution, and the number of beams in a row (of 2D beam array). To analyze the effectiveness of the proposed writing method in reducing the exposing time, the number of empty cycles in the conventional writing methods is derived under various conditions. The new writing method is applicable to both uniform and nonuniform dose distributions. In another method to reduce the exposing time in the case of nonuniform dose distribution, the maximum dose among the regions of a feature is decreased and the doses in the nearby regions are increased to reduce the dose difference among the regions as much as possible while maintaining the PEC result acceptable. This procedure increases the utilization of beams resulting in a shorter exposing time. These two methods may be combined to achieve even a larger reduction of exposing time. In the performance analysis, in addition to the uniform dose distribution, three different types of nonuniform dose distributions within a feature, developed for the PEC in a previous study,[5] are considered, i.e., A-type, M-type, and V-type. In this article, the two methods are described, and the results from an extensive simulation are provided with the detailed analysis.

The rest of the article is organized as follows. The simulation model is depicted in Sec. II. In Sec. III, the conventional writing methods for the MPES are briefly reviewed. In Sec. IV, the methods for reducing the exposing time are described in detail. In Sec. V, the simulation setup is explained. In Sec. VI, the simulation results are discussed, followed by a summary in Sec. VII

II. MODEL

The model of MPES employed in this study is derived from the eMET[9] and MBM-1000[10] where beams are arranged in a 2D array of 512×512, the cross-section of a beam is a square of $10 \times 10\,\text{nm}^2$, and the beam energy is 50 KeV. The beams can be turned on or off individually, and beams are deflected in a synchronized manner, i.e., the same angle and direction.

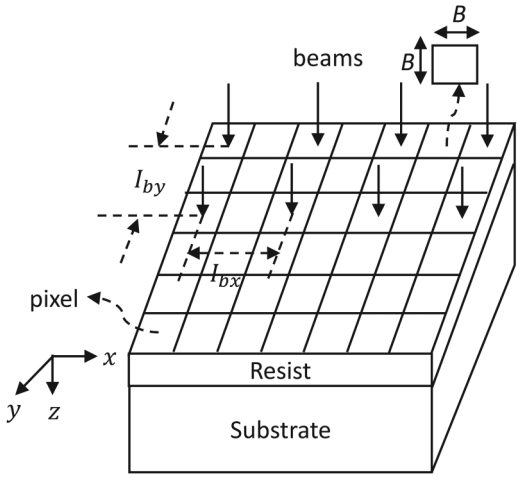

FIG. 1. Coordinate system employed in this study. The substrate moves in the X direction exposed by parallel beams: the beam size is $B \times B$, and the beam intervals are I_{bx} and I_{by} in the x and y dimensions, respectively.

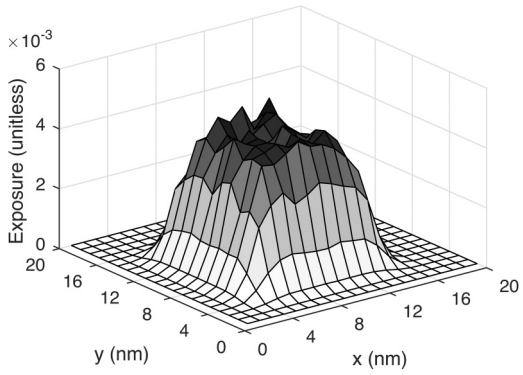

FIG. 2. Transfer function for the beam size of $10 \times 10\,\text{nm}^2$, i.e., $B = 10$ nm, with the noise level of 7%.

In a typical substrate system (Fig. 1), a resist layer is on the top of the substrate, where the X–Y plane corresponds to the top surface of the resist and the resist depth is along the Z-dimension. The resist layer to be exposed can be modeled as an array of square pixels with each pixel of size $B \times B$, the same as the beam size on the resist. B is set to 10 nm in this study. The exposing interval, I_{ex}, can be larger, smaller, or equal to B. For simplicity, it is assumed that $I_{ex} = B$.

The transfer function is denoted by TF (x, y, z), which describes the exposure distribution in the resist when a point (pixel) is exposed by a beam. Since the exposure in the resist is stochastic in nature, a stochastic transfer function is required to obtain realistic results. The TF (Fig. 2) is modeled by the convolution of an ideal TF (constant within the area of $B \times B$ and zero outside for all layers of resist) and a Gaussian function. The standard deviation σ_t of the Gaussian function refers to the *blurring factor*, which measures the level of beam blur and forward scattering of electrons. Then, a certain level of Gaussian noise is added to the (deterministic) transfer function to obtain the stochastic transfer function.[14]

Then, the 3D spatial distribution of exposure, $E(x, y, z)$, can be expressed by the following convolution:

$$E(x, y, z) = \int_{y'} \int_{x'} d(x - x', y - y') TF(x', y', z) dx' dy', \qquad (1)$$

where $d(x, y)$ represents the dose distribution to be given to a circuit pattern.

III. WRITING METHODS

The conventional writing methods, single-row writing[12] and multirow writing,[13] are briefly described in this section. The single-row writing is used in the eMET[9] and the multirow writing is developed for the MPES model derived from the eMET and

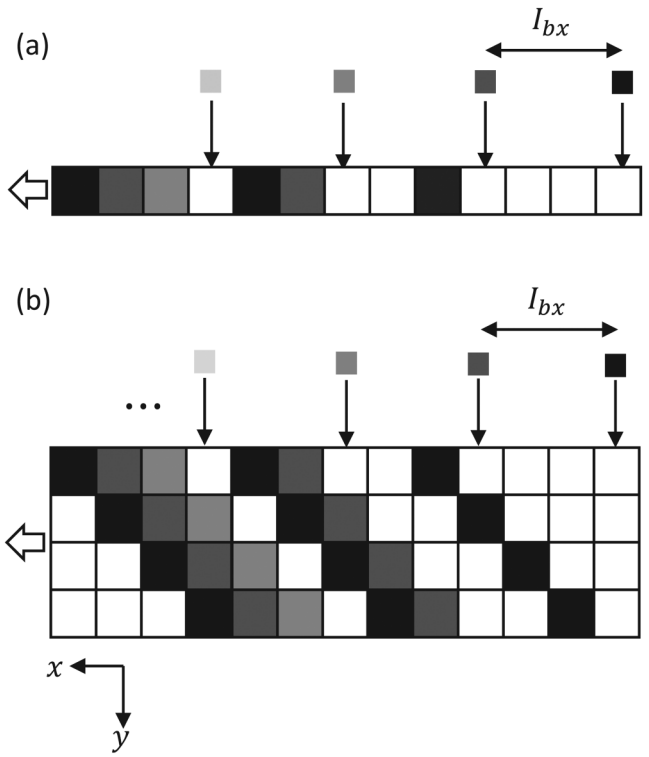

FIG. 3. Illustration of the single-row and multirow writing methods where larger and smaller squares represent pixels and beams, respectively, $I_{bx} = 3B$, and $n_s = 4$. (a) In the single row writing, a row of pixels are exposed by four beams, and (b) in the multi-row writing, four rows of pixels are exposed by four beams. In the multi-row writing method, each pixel is exposed by a beam once in a cycle; hence, the same writing pattern is repeated by the next beams in the row three more times to provide four shots to each pixel. In both figures, the substrate moves to the left and the pixels with the same shade of gray are exposed by the beam with the same shade. Each figure is a snapshot at the beginning of first step of a cycle.

MBM-1000.[10] The dose given to a pixel in a *step* is denoted by d and the beam interval, the distance between two adjacent beams, is expressed by I_{bx}. All beams in a system are controlled in a synchronized fashion.

In the single-row writing method [Fig. 3(a)], the writing path of each beam is on a single row of pixels. A beam or a group of beams exposes a pixel in the moving substrate, starting with with its vertical orientation, and gives a total (or target) dose of $D = n_s d$ to the pixel through n_s steps by deflecting in each step. The duration of n_s steps to give the target dose of D to each pixel is referred to as a *cycle*. After completing a cycle, the beam is reset back to its initial orientation and exposes another pixel in the next cycle. It is assumed that the time required to reset beams is negligible compared to a step. The condition of $n_s = \frac{I_{bx}}{B} + 1$ is maintained to achieve a uniform dose distribution without any hole in the exposed region.

In the multirow writing method [Fig. 3(b)], the writing path of each beam is over multiple rows of pixels. Each beam exposes a set of n_s pixels, each pixel once, distributed in both X and Y dimensions in each writing path. If the target dose for a pixel is $D = n_s d$, the pixel is exposed by n_s different beams in the same row. The spatial distribution of n_s pixels exposed by a beam is the same for all beams in a system.

IV. METHODS FOR REDUCING EXPOSING TIME

Two methods for increasing the utilization of beams and, therefore, reducing the exposing time are developed, i.e., (1) utilizing the cycles with all the beams turned off (empty cycles) and (2) lowering the dose difference among the regions of a feature in the PEC. The circuit pattern ("pattern" hereafter) considered in this study is assumed to consist of lines and spaces, i.e., a line/space pattern.

A. Writing method without empty cycle

In conventional (single-row and multirow) writing methods, the substrate moves continuously underneath the array of beams and each beam follows a pixel (single-row) or a set of pixels (multirow) by deflecting in each step during the $(\frac{I_{bx}}{B} + 1)$ steps of a cycle. Then, the beam is reset back to its vertical orientation and exposes another pixel or a set of pixels in the next cycle. When the target dose distribution in a pattern is nonuniform, all the beams may be turned off together in some cycles, i.e., empty cycles. The number of empty cycles depends on the widths of feature, i.e., line (l), space (s), and pattern, the target dose distribution, I_{bx}, and the number of beams (n) in a row.

To remove the empty cycles in the conventional writing method while realizing a dose distribution, the deflection angle of beams is adjusted in the proposed writing method such that the beams skip to the next cycle when at least one beam falls on a pixel requiring a dose. Figure 4 illustrates the idea of the proposed writing method. All the beams are turned off during the fourth cycle in the conventional (single-row) writing method [Fig. 4(a)], while the deflection angle of beams is adjusted during the fourth cycle in the proposed writing method to expose the next available pixels in the pattern [Fig. 4(b)]. The higher the number of empty cycles in the conventional writing method, the larger the reduction of exposing time by the proposed writing method.

In general, there are two possible states during the process of exposing a pattern, *transient* and *steady* states. The transient state occurs at the beginning and end of the exposure when all the beams are not over the pattern. On the other hand, the steady state occurs when all the beams are over the pattern. Suppose that m cycles are required to give the target dose distribution to the entire pattern in the conventional writing method. Due to the spaces between features and some pixels not requiring any dose based on the shape of the dose distribution, all the beams in the system are turned off in some cycles. By tracing the writing method through simulation, the number of empty cycles in the conventional writing method, denoted as m_ϕ, can be determined. In the proposed writing method, each empty cycle is skipped to the next available nonempty cycle by changing the initial vertical orientation ($\theta = 0$) to an angle θ. Therefore, the number of cycles required to give the target dose distribution to the entire pattern in the proposed writing method is $(m - m_\phi)$.

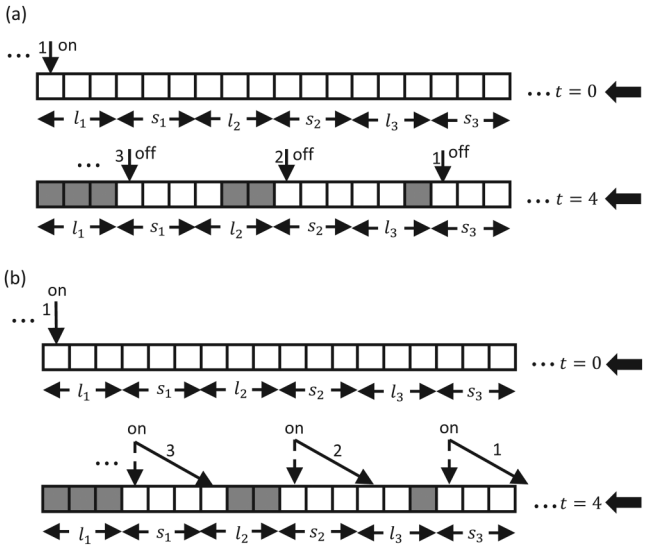

FIG. 4. Comparison of the writing methods: (a) the conventional (single-row) writing method, and (b) the proposed writing method. The solid arrows with numbers indicate the orientation of beams and the squares represent a row of pixels. More beams become visible (in the figure) exposing the pixels as the substrate moves to the left. The gray and white squares represent the exposed and unexposed pixels, respectively; l_i is the width of feature (line) i; and s_i is the space between two adjacent features, i.e., features i and $i+1$, in a line/space pattern where $l_i = l_j$ and $s_i = s_j$.

The percent reduction of exposing time by the proposed writing method with respect to the conventional writing method is denoted by t_{red}, which is computed as the ratio of the difference in the number of required cycles between the two writing methods to the number of cycles required by the conventional writing method, i.e.,

$$t_{red} = \frac{m - (m - m_\phi)}{m} \times 100\% = \frac{m_\phi}{m} \times 100\%. \tag{2}$$

It needs to be noted that in the case of line/space pattern, the ratio of $\frac{m_\phi}{m}$ can be determined from one row of pixels since the same dose distribution is to be achieved in all the rows.

B. Reduction of dose difference among the regions

In our previous work,[15] the shape+dose control for the PEC was implemented through an iterative procedure to find the optimal linewidth reduction, ΔW, and the optimal spatial-dose-distribution ratio. To have a sufficient spatial control of dose distribution, the line feature is partitioned into five regions along its length dimension. However, the higher the dose difference among the regions, the lower the beam utilization and, therefore, the longer the exposing time. After finding the optimal dose-distribution ratio, the difference in doses among the regions is carefully reduced by lowering the maximum dose among the five regions by a certain amount and distributing that amount to the nearby regions evenly so that beam utilization is increased, and hence, the exposing time is reduced, as illustrated in Fig. 5. The cost function to be optimized, C, consists of four metrics, i.e., the critical dimension (CD) error, line edge roughness (LER), total dose, and the beam utilization U,

$$C = a_1 CD\_error_{norm} + a_2 LER_{norm} + a_3 total\_dose_{norm} + a_4 \frac{1}{U_{norm}}, \tag{3}$$

where a_1, a_2, a_3, and a_4 are the weights given to the normalized CD error, LER, total dose, and $\frac{1}{U}$, respectively.

The total dose is the integration of area dose over the feature width. The beam utilization, U, is defined as the fraction of time the beams are on with respect to the total exposing time. The ranges and units of the metrics in the cost function are different. Therefore, the metrics are normalized so that they are on the same scale as follows:

$$\tilde{X} = \frac{X - X_{\min}}{X_{range}}, \tag{4}$$

where X is a metric, $X_{\min}$ is the minimum of X, X_{range} is the difference between the maximum and minimum of X, and $\tilde{X}$ is the normalized metric.

In the optimization procedure, the optimal dose for each region of a feature is searched for between $d_{\min\_allowed}$ and $d_{\max\_allowed}$, where $d_{\min\_allowed}$ and $d_{\max\_allowed}$ are the minimum

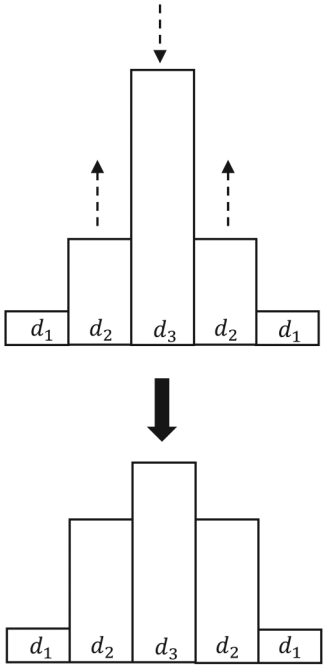

FIG. 5. Dose difference among the five regions may be decreased to improve beam utilization and reduce the exposing time: an illustration for the dose distribution of A-type.

and maximum doses allowed in a region of the feature, respectively. The $d_{\min\_allowed}$ is selected at which the CD of the feature is smaller than the target CD, and $d_{\max\_allowed}$ is set to be an integer multiple of $d_{\min\_allowed}$. Suppose that the CD error is α (nm) and the LER is β (nm) when all regions of the feature are given the same dose $d_{\min\_allowed}$. Then, α and β are taken as the maximum CD error and LER, respectively. The minimum CD error and LER are 0. The minimum beam utilization is obtained when one of the regions in a feature receives the dose $d_{\max\_allowed}$ and the rest receive the dose $d_{\min\_allowed}$. The maximum beam utilization is 1.

The optimal reduction of dose difference among the five regions of a feature is determined through an iterative procedure such that the cost function in Eq. (3) is minimized. The following notations are used in the description of the procedure.

$C_{\min}$: The minimum value of cost function.
$\{d_i\}$: The spatial dose distribution where d_i is the dose for region i.
Δd_i: The amount of adjustment for d_i. $\Delta d_i = d_i \times x$, where $0 < x < 1$.
$\{d_i\}_{opt}$: The optimal spatial dose distribution.
$d_{\max}$: The maximum dose among the regions of a feature.

The iterative procedure to reduce the dose difference among the regions of a feature is described below, where k is the iteration index, and its flowchart is also provided in Fig. 6.

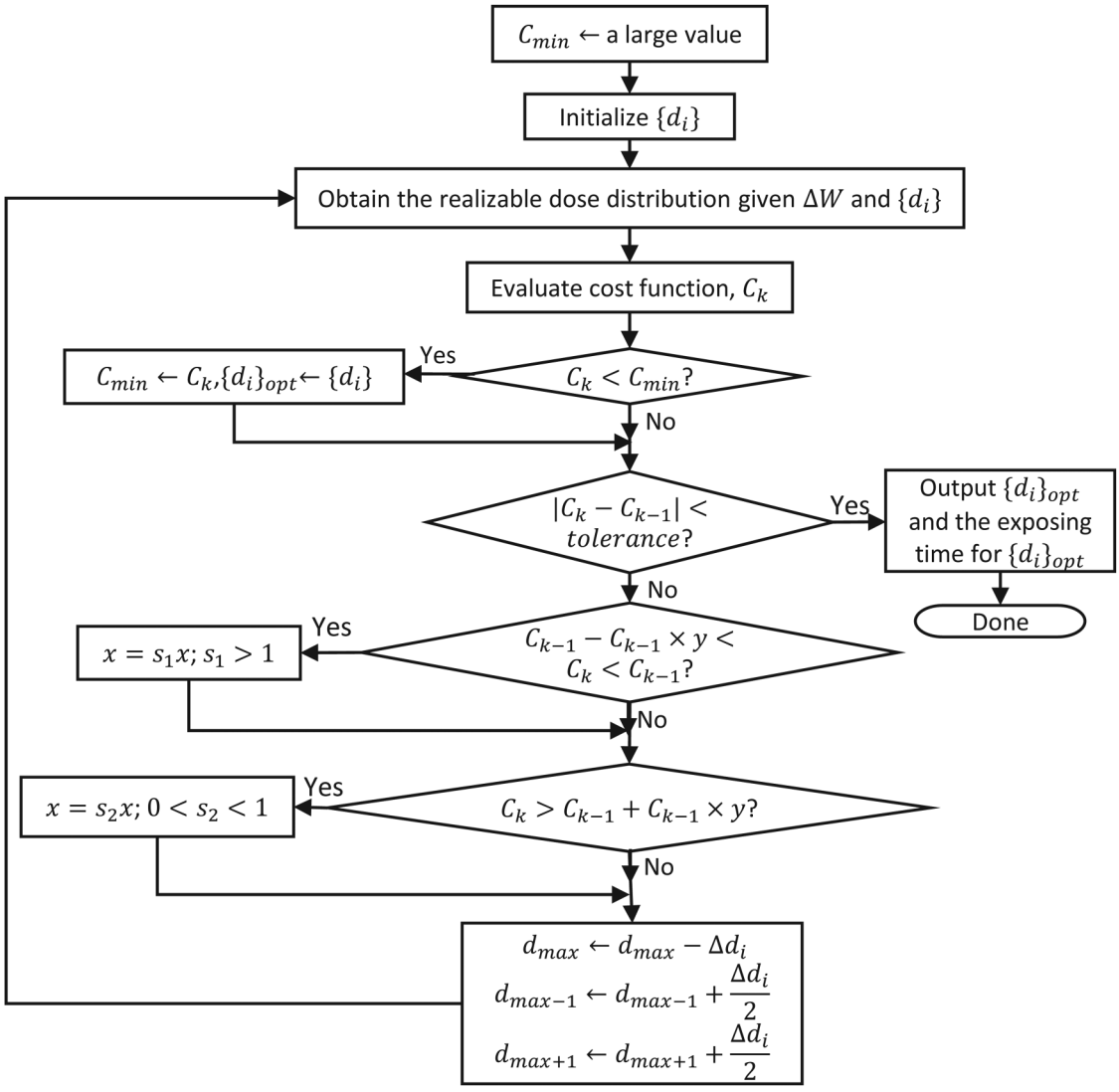

FIG. 6. Flowchart of decreasing dose difference among the regions of a feature to improve the beam utilization and reduce the exposing time where k is the iteration index, $0 < x < 1$, and $0 < y < 1$.

1. $C_{\min} \leftarrow$ a large value.
2. Initialize $\{d_i\}$ with the optimal dose distribution obtained by the shape+dose correction method.[15]
3. Obtain the realizable dose distribution given the optimal ΔW and $\{d_i | i = 1, 2, 3, 4, 5\}$.
4. Evaluate the cost function, C_k.
5. If $C_k < C_{\min}$,

$$C_{min} \leftarrow C_k, \text{ and } \{d_i\}_{opt} \leftarrow \{d_i\}.$$

6. If $| C_k - C_{k-1} | < tolerance$, go to step 10.
7. If $C_{k-1} - C_{k-1} \times y < C_k < C_{k-1}$ where $0 < y < 1$, i.e., the improvement in C is too small,

$$x \leftarrow s_1 x (s_1 > 1).$$

8. If $C_k > C_{k-1} + C_{k-1} \times y$,

$$x \leftarrow s_2 x \, (0 < s_2 < 1).$$

9. $d_{\max} \leftarrow d_{\max} - \Delta d_i$ maintaining $d_{\max}$ the maximum of the doses among the five regions and Δd_i is evenly distributed to the nearby regions. Go to step 3.
10. Output $\{d_i\}_{opt}$ and the exposing time required for $\{d_i\}_{opt}$.

V. SIMULATION

The effectiveness of the proposed methods to reduce the exposing time has been analyzed through simulation. The TF is modeled based on the 3D point spread function (PSF) generated using a Monte Carlo simulation program CASINO[16] for the substrate system of 100 nm PMMA on Si, the beam energy of 50 keV, and the beam diameter of 6 nm. The total exposure and forward scattering range (the standard deviation of Gaussian) are extracted from the PSF for each of the five resist layers. The ratios of the total energy and forward scattering range among the five resist layers are referred to in setting the total exposure and σ_t of the Gaussian function used to generate the TF of each layer.

The 3D exposure distribution in the resist is computed at the resolution I_{sm}, referred to as simulation interval, which is set to $\frac{1}{2}$ nm. The developing-rate distribution is derived from the exposure distribution and then the remaining resist profile is obtained through a fast path-based resist-development simulation.[17] The development simulation continues until the feature is fully developed to the bottom layer of the resist. The cross-section and top–down views of the remaining resist profile, from which the CD and LER are measured, are illustrated in Fig. 7. The CD error is quantified as the absolute difference between the target and actual feature (line) widths, and LER as the standard deviation of actual feature edge location along the length dimension of a feature, both averaged over the top, middle, and bottom layers. The middle 80% segment of the developed feature along the length dimension is used in the computation of CD and LER to exclude the edge effect (rounding at corners).

In analyzing the percent reduction of exposing time, t_{red}, by the proposed writing method, the widths of feature (l), space (s), and pattern are varied while the beam interval I_{bx} is kept at 100 nm. The numbers of cycles and empty cycles in the conventional writing

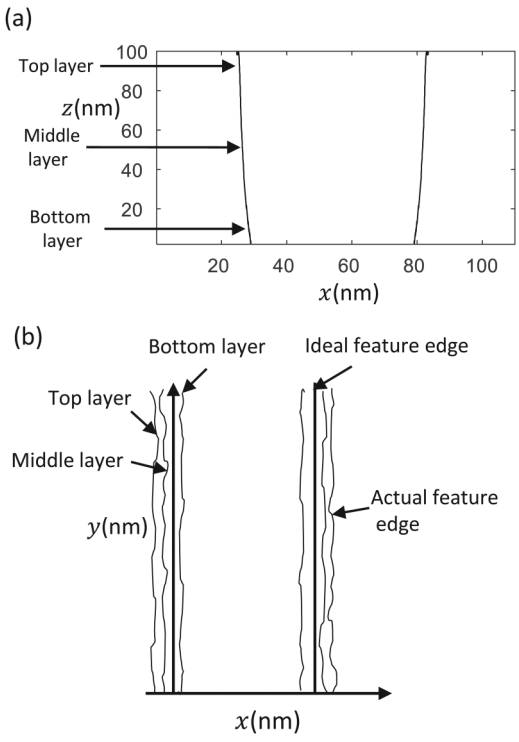

FIG. 7. Remaining resist profile of a line feature: (a) the cross-section view where the three layers are shown and (b) the top–down view where actual feature boundaries (edges) on the three layers are shown. The feature size is 50×300 nm^2 and the resist thickness is 100 nm.

method are calculated by tracing the writing procedure on the entire pattern through simulation. Then, t_{red} is calculated using Eq. (2). Given a beam interval I_{bx} and $n\left(\frac{I_{bx}}{B} + 1\right)$ beams in a row, the cycles to expose the first $\frac{I_{bx}}{B} \times \frac{I_{bx}}{B}$ pixels by the first $\left(\frac{I_{bx}}{B} + 1\right)$ beams are repeated in the steady state by the next $\left(\frac{I_{bx}}{B} + 1\right)$ beams to expose the next $\frac{I_{bx}}{B} \times \frac{I_{bx}}{B}$ pixels, and so on. Therefore, for simplicity, the case of $\left(\frac{I_{bx}}{B} + 1\right)$ beams in a row is considered.

In observing the effectiveness of lowering the dose difference among the regions in reducing the exposing time, two different feature sizes (linewidths), i.e., 50 and 150 nm, are considered with the feature length fixed at 300 nm. Both sharp and broad TFs are considered, i.e., $\sigma_t = 1$ nm and 4 nm. The features are corrected for the proximity effect with four types of dose distributions, i.e., uniform, V-type, M-type, and A-type.[5] It was shown previously that the A-type dose distribution is effective when the aspect ratio (resist thickness to feature width) is relatively large while the uniform or V-type distribution tends to work better for a relatively small aspect ratio. In our previous study,[15] a systematic method for realizing various types of spatial dose distributions with an arbitrary reduction of feature size on an MPES was developed. The method utilizes multipass writing, i.e., exposes each writing path multiple times, to increase the dose range and/or dose resolution. The point of exposure on the substrate for each beam is shifted by the amount of $\frac{\Delta W}{2}$

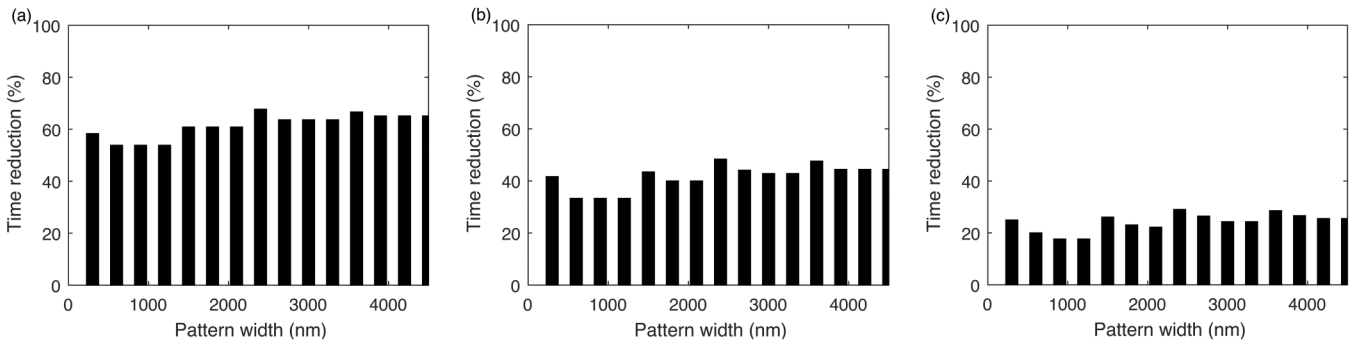

FIG. 8. Reduction of exposing time by the proposed writing method, t_{red}, when $l_{bx} = l + s$, $l_i = l_j$, $l_{bx} = 100$ nm, the dose distribution is uniform and (a) $l = 30$ nm, (b) $l = 50$ nm, and (c) $l = 70$ nm.

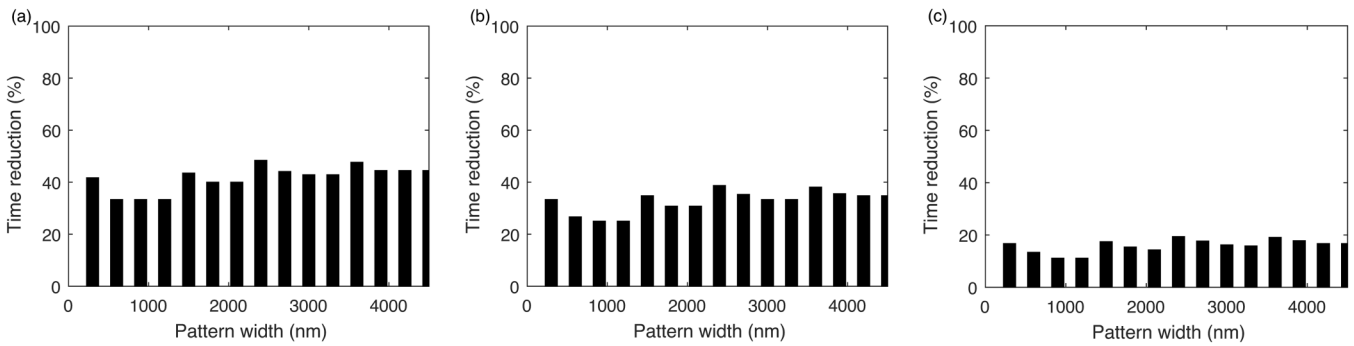

FIG. 9. Reduction of exposing time by the proposed writing method, t_{red}, when $l_{bx} = l + s$, $l_i \neq l_j$, $l_{bx} = 100$ nm, the dose distribution is uniform and (a) $l_1 = 10$ nm, $l_2 = 30$ nm, $l_3 = 50$ nm; (b) $l_1 = 40$ nm, $l_2 = 50$ nm, $l_3 = 60$ nm; and (c) $l_1 = 60$ nm, $l_2 = 70$ nm, $l_3 = 80$ nm.

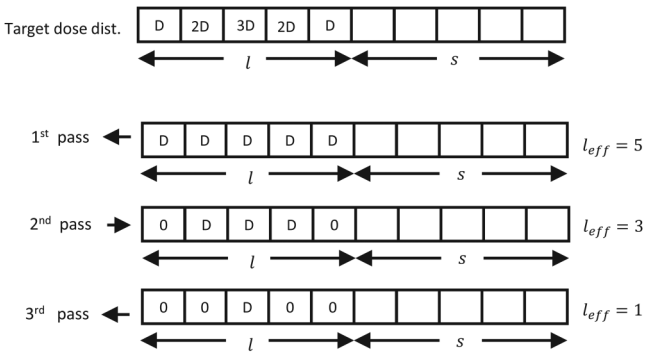

FIG. 10. Realization of a nonuniform dose distribution in multiple passes where the feature is divided into five regions and each region consists of a pixel with size $10 \times 10\,\text{nm}^2$. Each region may consist of more than a pixel.

(which is the width reduction on each side of line feature) in the direction of the substrate in each pass. Another benefit of using multipass is to spread the negative effects of abnormal beams spatially.[14]

The weights (a_1, a_2, a_3, and a_4) in the cost function are selected according to the relative importance of each metric. In this study, a_1, a_2, a_3, and a_4 are selected to be 1, 0, 0.2, and 0.5, respectively. Also, a_2 is set to 0 since the effect of the LER is not significant in any type of dose distribution as long as $\Delta W > 0$. As the main objective of the PEC is to minimize the CD error, the weight of the CD error (a_1) is five times larger than that of the total dose and two times larger than that of U. In the iterative optimization procedure, $x = 0.5$ initially, $s_1 = 2$, $s_2 = 0.5$, $y = 0.01$, and $tolerance = 0.005$. In each iteration, the doses of feature regions, $\{d_i\}$, are adjusted at the resolution of one-tenth of the nominal dose, which is the dose at which the CD error is not greater than 10 nm at any of the top, middle, and bottom layers. In calculating

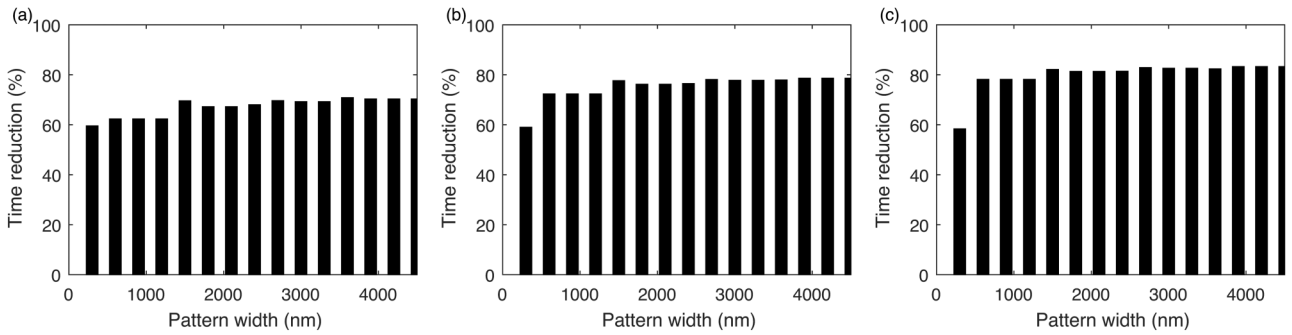

FIG. 11. Reduction of exposing time by the proposed writing method, t_{red}, when $l_{bx} = l + s$, $l_i = l_j$, $l_{bx} = 100$ nm, $l = 50$ nm, $s = 50$ nm and the dose distribution ratio is (a) 1:3:5:3:1, (b) 1:2:7:2:1, and (c) 1:1:9:1:1.

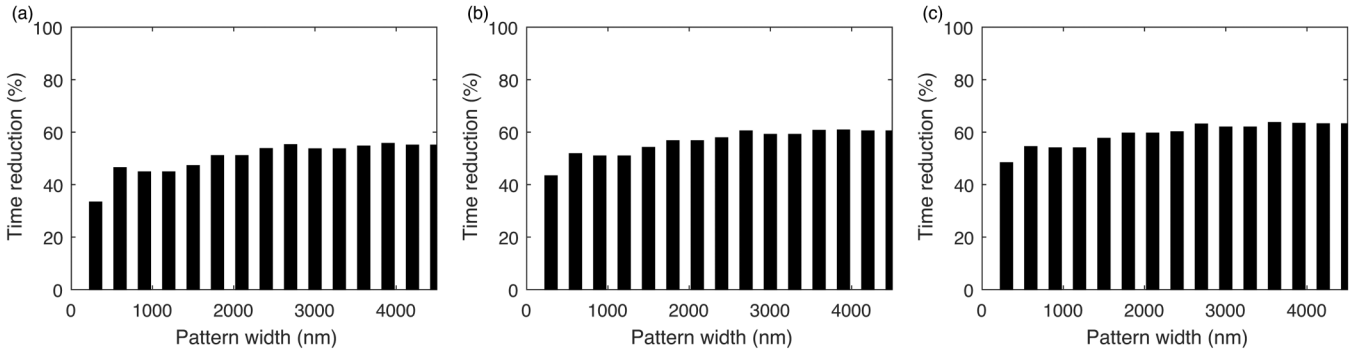

FIG. 12. Reduction of exposing time by the proposed writing method, t_{red}, when $l_{bx} = l + s$, $l_i \neq l_j$, $l_{bx} = 100$ nm, $l_1 = 40$ nm, $l_2 = 50$ nm, $l_3 = 60$ nm, and the dose distribution ratios for l_1, l_2, and l_3 are (a) 1:2:2:1, 1:1:2:1:1, and 1:1:1:1:1:1:1, respectively; (b) 1:4:4:1, 1:2:4:2:1, and 1:2:2:2:2:1, respectively; and (c) 1:8:8:1, 1:4:8:4:1, and 1:4:4:4:4:1, respectively.

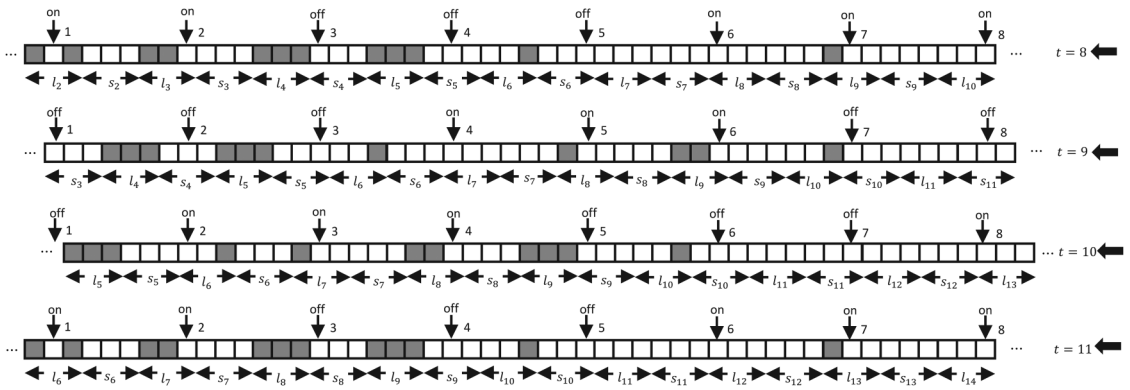

FIG. 13. Tracing the pixels exposed by the beams in multiple cycles in the steady state for the conventional writing method when $l_{bx} > l + s$ and $l_i = l_j$. In this figure, $l_{bx} = 70$ nm, $l = 30$ nm, and $s = 30$ nm. The gray and white squares represent the exposed and unexposed pixels, respectively.

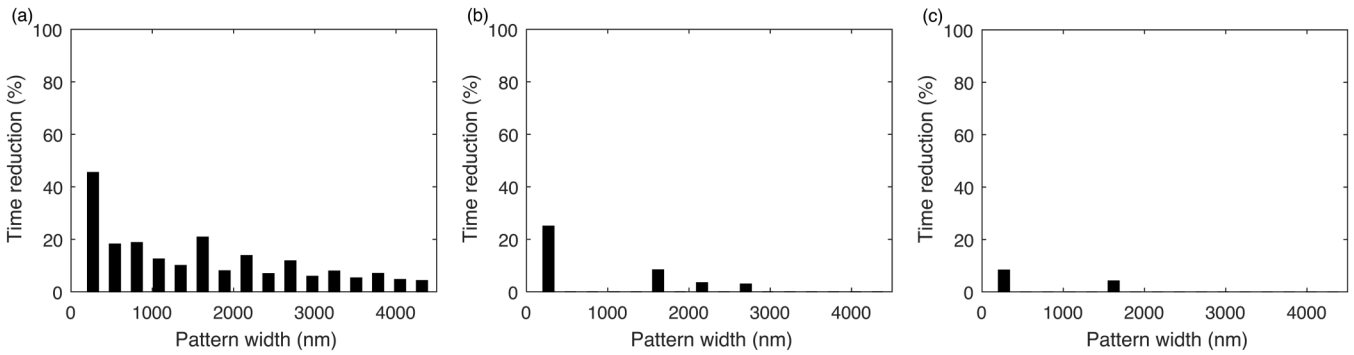

FIG. 14. Reduction of exposing time by the proposed writing method, t_{red}, when $I_{bx} \neq l + s$, $l_i = l_j$, $I_{bx} = 100$ nm, $s = 40$ nm, the dose distribution is uniform and (a) $l = 30$ nm, (b) $l = 50$ nm, and (c) $l = 70$ nm.

the exposing time, the following parameters are assumed: $I_{bx} = 100$ nm (beam interval), $n = 11$ (the number of beams per row, $n = \frac{I_{bx}}{B} + 1$), $s = 40$ nm (space width) when $I_{bx} \neq l + s$, $d = 0.1$ (dose per step), and pattern width of 4.5 μm.

VI. RESULTS AND DISCUSSION

The results are presented in two parts. First, the percent reduction of exposing time by the proposed writing method compared to conventional writing methods is examined with the pattern width varied. Note that the exposing time is the same for the single-row and multirow writing methods. Hence, the single-row writing method is used as the conventional writing method to compare in this study. Then, the results without and with PEC are compared varying the feature size, the blurring factor of TF, and the dose distribution type. The PEC results include both cases of applying and not applying the method of reducing the dose difference among the regions of a feature.

When the feature (l) and space (s) widths vary within a pattern, the notations l_i and s_i are adopted to distinguish different features and spaces, respectively.

A. Reduction of exposing time by removing empty cycles

To analyze the percent reduction of exposing time, t_{red}, by the proposed writing method, various cases are considered, which are presented in two parts, nonvarying and varying total dose from feature to feature. Each part considers the relationship among I_{bx}, l and s, i.e., $I_{bx} = l + s$ and $I_{bx} \neq l + s$, and different dose distribution types, i.e., uniform and nonuniform dose distributions. In a uniform dose distribution, the same dose is given to all regions of a feature, and in a nonuniform dose distribution, different doses are given to different regions of a feature.

In each case, t_{red} is plotted against the pattern width (size). In the transient state, the number of empty cycles and, hence, t_{red} can fluctuate significantly. A wide range of pattern size (width) is considered so that the behavior of t_{red} in both transient and steady states can be observed.

1. Nonvarying total dose from feature to feature

a. $I_{bx} = l + s$: Uniform dose distribution. The percent reduction of exposing time, t_{red}, by the proposed writing method in the case of $I_{bx} = l + s$, $l_i = l_j$, and uniform dose distribution is provided in Fig. 8. It is observed that t_{red} is proportional to s, the space between adjacent features. In this case, all the beams fall on the pixels that have the same positions in their respective features. Hence, in the conventional writing method, when the beams fall on the spaces, they are turned off together [see Fig. 4(a)]. As a result, all the beams are turned off $\frac{s}{I_{bx}}$ of the total exposing time. In the proposed writing method, when the beams fall on the spaces, the deflection angle of the beams is adjusted to expose the pixels requiring doses [see Fig. 4(b)]. As a result, the beams are always on. Hence, in the steady state, t_{red} is proportional to s and can be expressed as in Eq. (5),

$$t_{red} = \frac{I_{bx} - l}{I_{bx}} \times 100\% = \frac{s}{I_{bx}} \times 100\%. \tag{5}$$

In Fig. 9, t_{red} in the case of $I_{bx} = l + s$, $l_i \neq l_j$ and uniform dose distribution is provided. It is seen that t_{red} is proportional to the

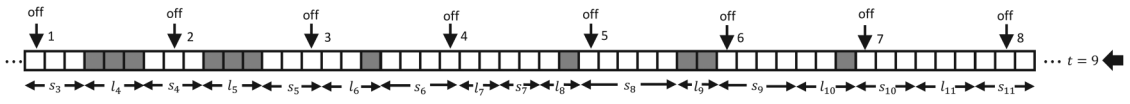

FIG. 15. Tracing the pixels exposed by the beams in the second cycle of the steady state for the conventional writing method when $I_{bx} > l + s$ and $l_i \neq l_j$. The gray and white squares represent the exposed and unexposed pixels, respectively.

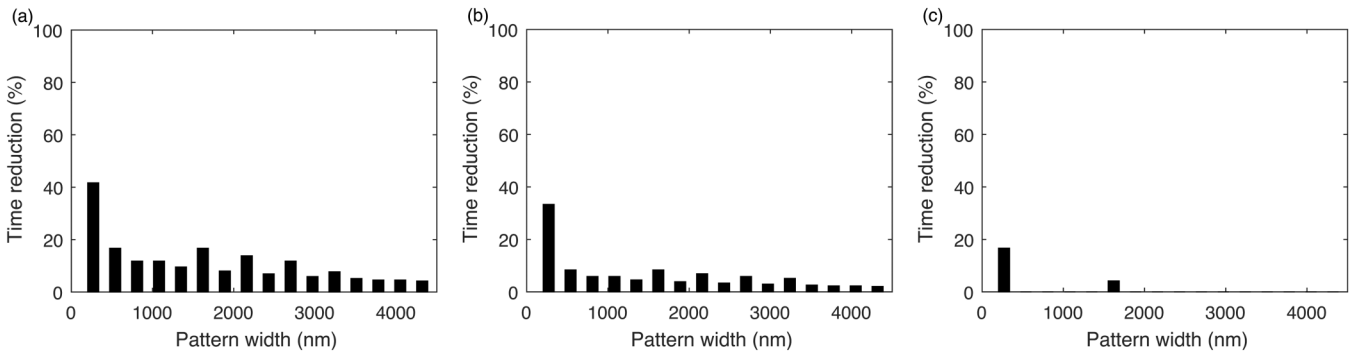

FIG. 16. Reduction of exposing time by the proposed writing method, t_{red}, when $l_{bx} \neq l + s$, $l_i \neq l_j$, $l_{bx} = 100$ nm, $l + s = 90$ nm, the dose distribution is uniform and (a) $l_1 = 10$ nm, $l_2 = 30$ nm, $l_3 = 50$ nm; (b) $l_1 = 40$ nm, $l_2 = 50$ nm, $l_3 = 60$ nm; and (c) $l_1 = 60$ nm, $l_2 = 70$ nm, $l_3 = 80$ nm.

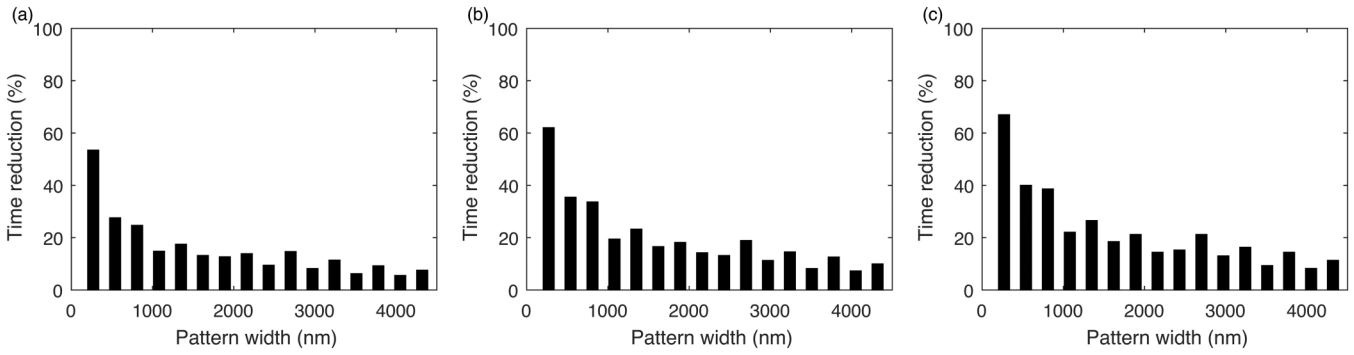

FIG. 17. Reduction of exposing time by the proposed writing method, t_{red}, when $l_{bx} \neq l + s$, $l_i = l_j$, $l_{bx} = 100$ nm, $l = 50$ nm, $s = 40$ nm and the dose distribution ratio is (a) 1:3:5:3:1, (b) 1:2:7:2:1, and (c) 1:1:9:1:1.

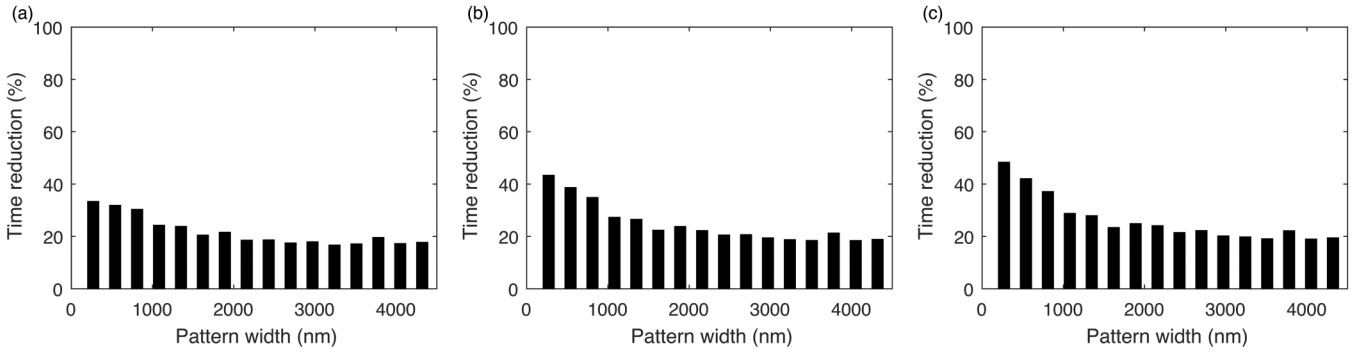

FIG. 18. Reduction of exposing time by the proposed writing method, t_{red}, when $l_{bx} \neq l + s$, $l_i \neq l_j$, $l_{bx} = 100$ nm, $l + s = 90$ nm, the dose distribution is non-uniform, $l_1 = 40$ nm, $l_2 = 50$ nm, and $l_3 = 60$ nm, and the dose distribution ratios for l_1, l_2, and l_3 are (a) 1:2:2:1, 1:1:2:1:1, and 1:1:1:1:1:1:1, respectively; (b) 1:4:4:1, 1:2:4:2:1, and 1:2:2:2:2:1, respectively; and (c) 1:8:8:1, 1:4:8:4:1, and 1:4:4:4:4:1, respectively.

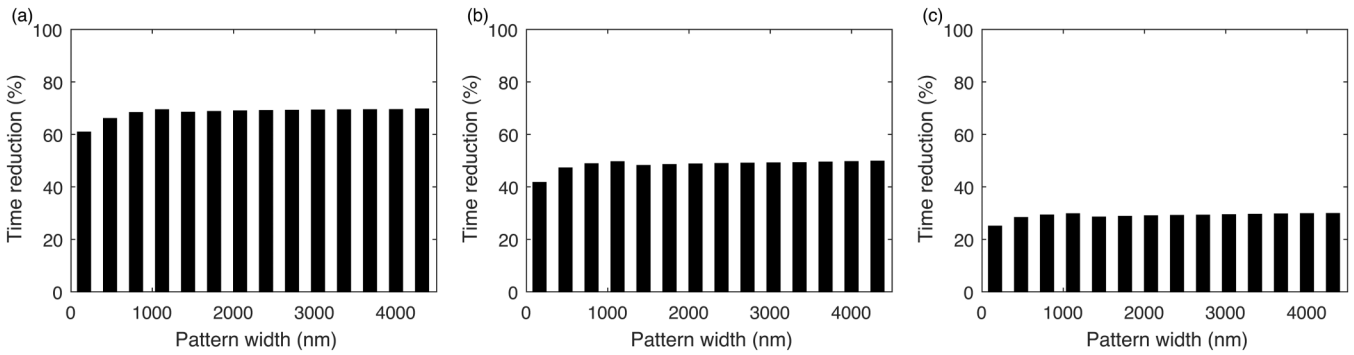

FIG. 19. Reduction of exposing time by the proposed writing method, t_{red}, when $l_{bx} = l + s$, $l_i = l_j$, $l_{bx} = 100$ nm, the dose distribution is uniform, and the feature-wise dose level varies linearly from the center toward the edge of pattern where the dose level at the edge is 1.5 times that at the center: (a) $l = 30$ nm, (b) $l = 50$ nm, and (c) $l = 70$ nm.

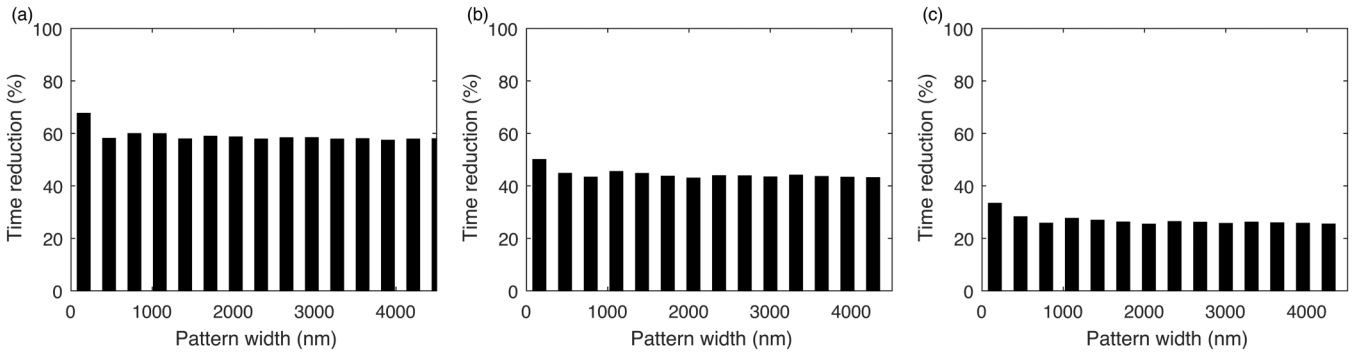

FIG. 20. Reduction of exposing time by the proposed writing method, t_{red}, when $l_{bx} = l + s$, $l_i \neq l_j$, $l_{bx} = 100$ nm, the dose distribution is uniform, and the feature-wise dose level varies linearly from the center toward the edge of pattern where the dose level at the edge is 1.5 times that at the center: (a) $l_1 = 10$ nm, $l_2 = 30$ nm, $l_3 = 50$ nm; (b) $l_1 = 40$ nm, $l_2 = 50$ nm, $l_3 = 60$ nm; and (c) $l_1 = 60$ nm, $l_2 = 70$ nm, $l_3 = 80$ nm.

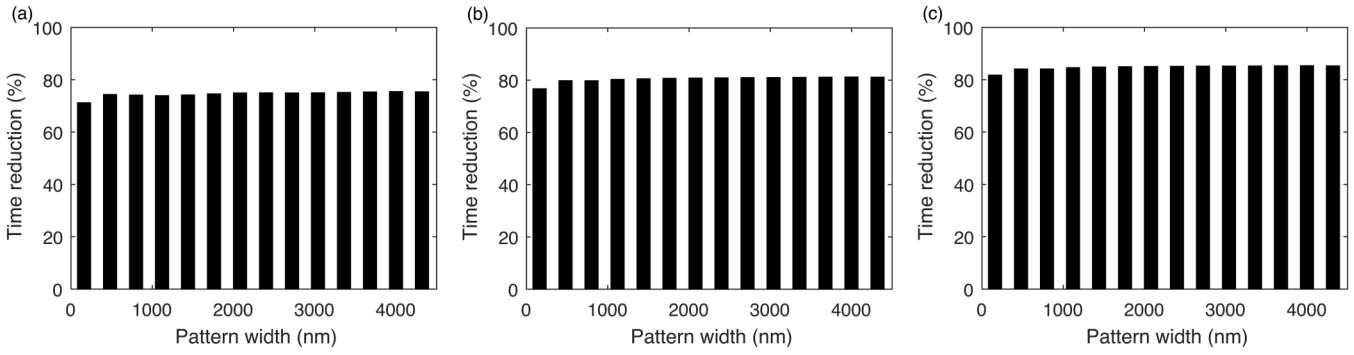

FIG. 21. Reduction of exposing time by the proposed writing method, t_{red}, when $l_{bx} = l + s$, $l_i = l_j$, $l_{bx} = 100$ nm, $l = 50$ nm, $s = 50$ nm, and the feature-wise dose level varies linearly from the center toward the edge of pattern where the dose level at the edge is 1.5 times that at the center: the dose distribution ratio in each feature is (a) 1:3:5:3:1, (b) 1:2:7:2:1, and (c) 1:1:9:1:1.

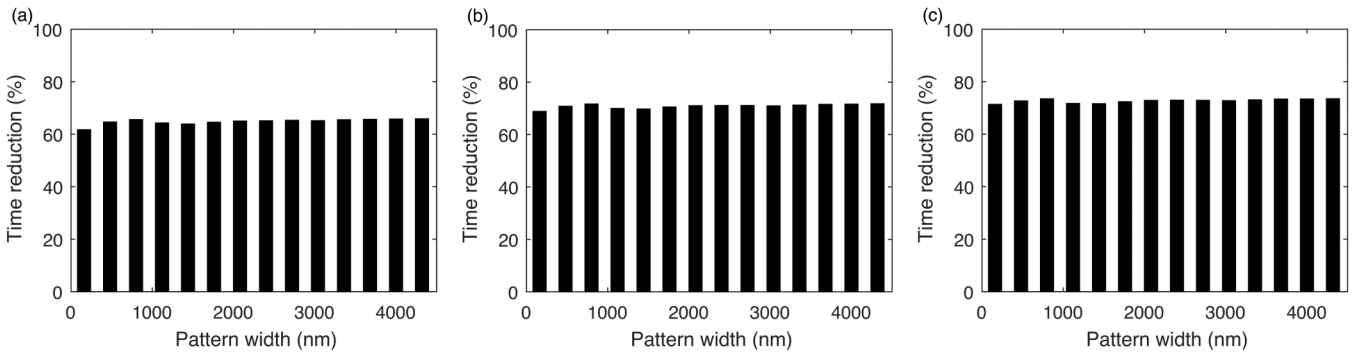

FIG. 22. Reduction of exposing time by the proposed writing method, t_{red}, when $l_{bx} = l + s$, $l_i \neq l_j$, $l_{bx} = 100$ nm, $l_1 = 40$ nm, $l_2 = 50$ nm, $l_3 = 60$ nm, and the feature-wise dose level varies linearly from the center toward the edge of pattern where the dose level at the edge is 1.5 times that at the center: the dose distribution ratios for l_1, l_2, and l_3 are (a) 1:2:2:1, 1:1:2:1:1, and 1:1:1:1:1:1:1, respectively; (b) 1:4:4:1, 1:2:4:2:1, and 1:2:2:2:2:1, respectively; and (c) 1:8:8:1, 1:4:8:4:1, and 1:4:4:4:4:1, respectively.

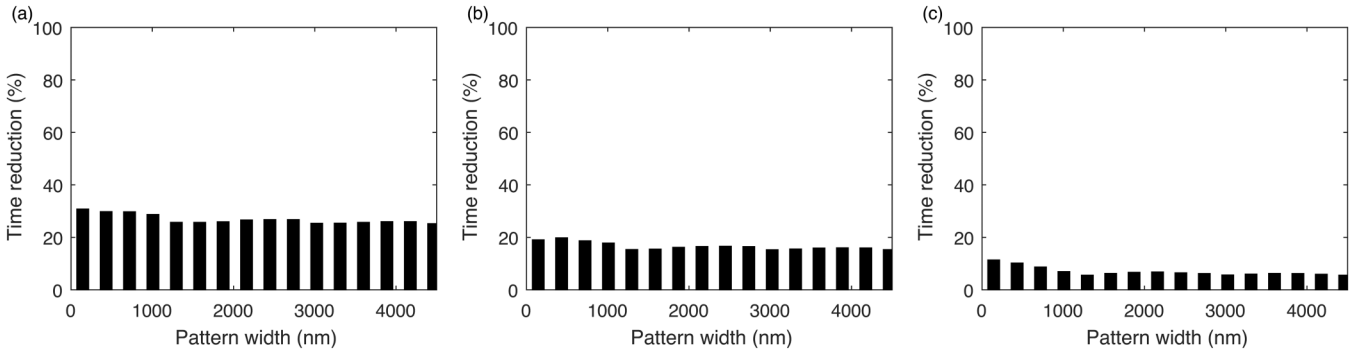

FIG. 23. Reduction of exposing time by the proposed writing method, t_{red}, when $l_{bx} \neq l + s$, $l_i = l_j$, $l_{bx} = 100$ nm, $l + s = 90$ nm, the dose distribution is uniform, and the feature-wise dose level varies linearly from the center toward the edge of pattern where the dose level at the edge is 1.5 times that at the center: (a) $l = 30$ nm, (b) $l = 50$ nm, and (c) $l = 70$ nm.

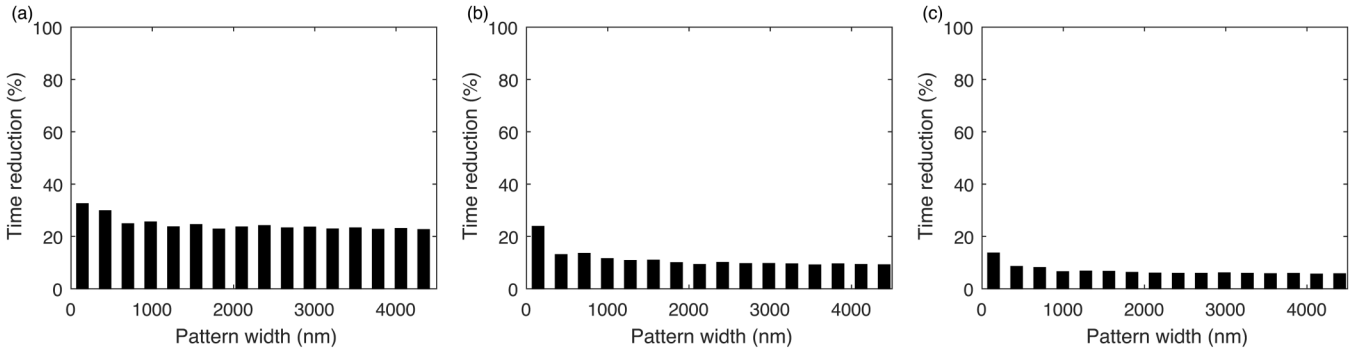

FIG. 24. Reduction of exposing time by the proposed writing method, t_{red}, when $l_{bx} \neq l + s$, $l_i \neq l_j$, $l_{bx} = 100$ nm, $l + s = 90$ nm, the dose distribution is uniform, and the feature-wise dose level varies linearly from the center toward the edge of pattern where the dose level at the edge is 1.5 times that at the center: (a) $l_1 = 10$ nm, $l_2 = 30$ nm, $l_3 = 50$ nm; (b) $l_1 = 40$ nm, $l_2 = 50$ nm, $l_3 = 60$ nm; and (c) $l_1 = 60$ nm, $l_2 = 70$ nm, $l_3 = 80$ nm.

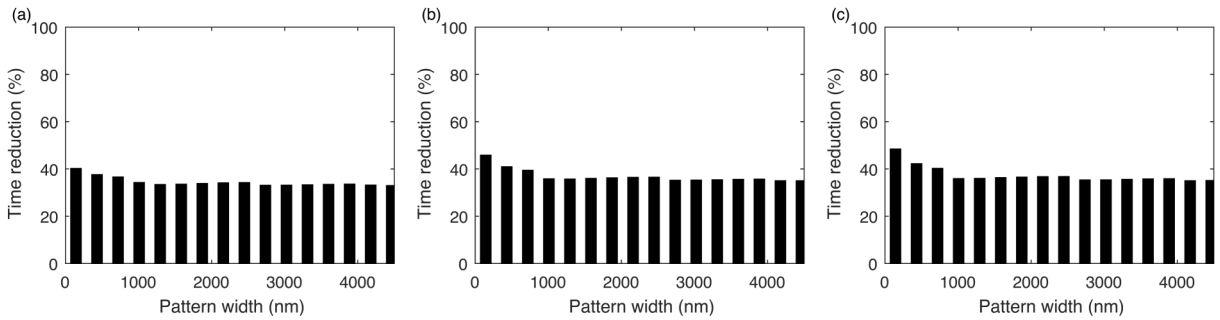

FIG. 25. Reduction of exposing time by the proposed writing method, t_{red}, when $l_{bx} \neq l + s$, $l_i = l_j$, $l_{bx} = 100$ nm, $l = 50$ nm, $s = 40$ nm, and the feature-wise dose level varies linearly from the center toward the edge of pattern where the dose level at the edge is 1.5 times that at the center: the dose distribution ratio in each feature is (a) 1:3:5:3:1, (b) 1:2:7:2:1, and (c) 1:1:9:1:1.

smallest s, i.e., $s_{\min}$. In this case, at least one beam is turned on $\frac{l_{\max}}{I_{bx}}$ of the total exposing time in the conventional writing method since each beam falls on the same position in its corresponding $(l + s)$ domain. Hence, all the beams are turned off together $\frac{s_{\min}}{I_{bx}}$ of the total exposing time in the conventional writing method. In the proposed writing method, the empty cycles are removed. Therefore, in the steady state, t_{red} is proportional to s_{min} and can be calculated as in Eq. (6),

$$t_{red} = \frac{I_{bx} - l_{\max}}{I_{bx}} \times 100\% = \frac{s_{\min}}{I_{bx}} \times 100\%. \tag{6}$$

b. $I_{bx} = l + s$: Nonuniform dose distribution. In the case of nonuniform dose distribution, the number of passes to achieve a target dose distribution is determined by the maximum dose, $d_{\max}$, required by a pixel. Also, some pixels in a feature may not require doses in each pass. The number of pixels in the feature requiring nonzero doses in each pass is referred to as *effective feature width*, denoted by l_{eff}. This is illustrated in Fig. 10, where the five pixels in the feature require the doses D, $2D$, $3D$, $2D$, and D, and three passes are used to achieve the target dose distribution. In the first pass, $l_{eff} = 5$, in the second pass, $l_{eff} = 3$, and in the third pass, $l_{eff} = 1$. As stated in Sec. VI A 1 "$I_{bx} = l + s$: Uniform dose distribution," when $I_{bx} = l + s$ and $l_i = l_j$, all the beams give doses to the pixels at the same positions in their respective features in the conventional writing method. Therefore, at least one beam is always on in l_{eff}/I_{bx} of the total cycles in each pass, and the beams are off together in the rest of the cycles. That is, a smaller l_{eff} in a pass leads to more empty cycles. Since empty cycles are removed in the proposed writing method, t_{red} in the steady state can be calculated

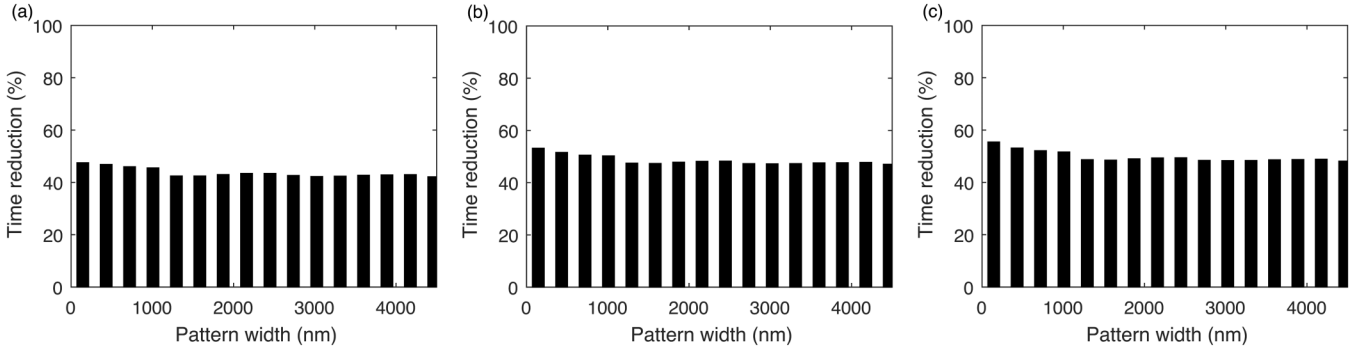

FIG. 26. Reduction of exposing time by the proposed writing method, t_{red}, when $l_{bx} \neq l + s$, $l_i \neq l_j$, $l_{bx} = 100$ nm, $l + s = 90$ nm, $l_1 = 40$ nm, $l_2 = 50$ nm, and $l_3 = 60$ nm, and the feature-wise dose level varies linearly from the center toward the edge of pattern where the dose level at the edge is 1.5 times that at the center: the dose distribution ratios for l_1, l_2, and l_3 are (a) 1:2:2:1, 1:1:2:1:1, and 1:1:1:1:1:1, respectively; (b) 1:4:4:1, 1:2:4:2:1, and 1:2:2:2:2:1, respectively; and (c) 1:8:8:1, 1:4:8:4:1, and 1:4:4:4:4:1, respectively.

as in the following equation:

$$t_{red} = \frac{N \times I_{bx} - \sum_{k=1}^{N} l_{eff_k}}{N \times I_{bx}} \times 100\% = \frac{\frac{d_{\max}}{D} \times I_{bx} - \sum_{k=1}^{\frac{d_{\max}}{D}} l_{eff_k}}{\frac{d_{\max}}{D} \times I_{bx}} \times 100\%, \quad (7)$$

where l_{eff_k} is the effective width of the feature in the kth pass and N is the number of passes ($N = \frac{d_{\max}}{D}$).

In Fig. 11, t_{red} is provided in the case of $I_{bx} = l + s$, $l_i = l_j$, and nonuniform dose distribution. It is seen that the higher the dose difference among the pixels in the feature, the larger t_{red}. This is because l_{eff_k} becomes smaller in the later passes compared to the first pass when the dose difference among the pixels is larger.

When $I_{bx} = l + s$ and $l_i \neq l_j$, t_{red} in the steady state depends on the largest l_{eff} among features in each pass, i.e., $l_{eff_{\max}}$. This is because at least one beam is turned on $\frac{l_{eff_{\max}}}{I_{bx}}$ of the total exposing time in each pass in the conventional writing method similar to the respective case ($I_{bx} = l + s$ and $l_i \neq l_j$) in Sec. VI A 1 "$I_{bx} = l + s$: Uniform dose distribution." Therefore, t_{red} in the steady state can

TABLE I. CD error, total dose, beam utilization, and exposing time by the conventional writing method, $t_{exp,old}$, and the proposed writing method, $t_{exp,new}$, for the three cases, i.e., no PEC optimization (no use of cost function), the PEC optimization without the method of reducing the dose difference (the rows with C), and the PEC optimization with the method of reducing the dose difference (the rows with C^*). $C = CD\_error_{norm} + 0.2 total\_dose_{norm} + 0.5\frac{1}{U_{norm}}$, $I_{bx} \neq l + s$, $s = 40$ nm, $I_{bx} = 100$ nm for $l = 50$ nm, and $I_{bx} = 200$ nm for $l = 150$ nm.

l (nm)	σ_t (nm)	Type	Cost function	ΔW (nm)	Dose ratio	CD error (nm)	Total dose (unitless)	U (%)	$t_{exp,old}$ (cycle)	$t_{exp,new}$ (cycle)
50	1	A	…	0	1:2:7:2:1	1.25	1.30	37.14	1881	1761
50	1	A	C	4	1:2.19:4.36:2.19:1	0.34	1.76	49.27	2084	1915
50	1	A	C^*	4	1:2.25:4.22:2.25:1	0.37	1.74	50.81	1940	1828
50	1	M	…	0	1:5:1:5:1	1.55	1.30	52.00	2542	2486
50	1	M	C	4	1:5.75:2.51:5.75:1	0.37	1.81	55.68	2763	2635
50	1	M	C^*	4	1:5.45:3.0:5.45:1	0.40	1.78	58.35	2641	2528
50	1	V	…	0	4:2:1:2:4	4.64	1.30	65.00	1663	1520
50	1	V	C	8	1.31:1.08:1:1.08:1.31	0.19	3.18	88.24	2668	2532
50	1	V	C^*	8	1.26:1.16:1:1.16:1.26	0.19	3.20	92.58	2618	2489
50	4	A	…	0	1:2:7:2:1	1.46	1.50	37.14	1780	1671
50	4	A	C	10	1:2.10:5.25:2.10:1	0.25	2.19	43.62	2520	2352
50	4	A	C^*	10	1:2.34:5.02:2.34:1	0.28	2.22	46.62	2369	2213
50	4	M	…	0	1:5:1:5:1	1.61	1.50	52.00	1995	1809
50	4	M	C	10	1:6.68:2.80:6.68:1	0.26	2.24	54.37	3249	3110
50	4	M	C^*	10	1:6.55:3.05:6.55:1	0.29	2.21	55.42	3115	2985
50	4	V	…	0	4:2:1:2:4	5.11	1.50	65.00	1493	1344
50	4	V	C	14	4.25:2.09:1:2.09:4.25	0.25	2.94	64.37	2154	2044
50	4	V	C^*	14	4.10:2.29:1:2.29:4.10	0.29	2.95	67.22	2050	1945
150	1	A	…	0	1:2:7:2:1	5.26	3.50	37.14	1916	1780
150	1	A	C	4	1:2.08:5.82:2.08:1	0.47	4.86	41.16	2718	2515
150	1	A	C^*	4	1:2.33:5.35:2.33:1	0.51	4.88	44.90	2508	2345
150	1	M	…	0	1:5:1:5:1	4.90	3.50	52.00	2248	2010
150	1	M	C	4	1:6.60:2.11:6.60:1	0.53	4.87	52.45	3225	3068
150	1	M	C^*	4	1:6.34:2.94:6.34:1	0.58	4.91	55.58	3059	2935
150	1	V	…	0	4:2:1:2:4	4.63	3.50	65.00	2110	1821
150	1	V	C	8	1.24:1.12:1:1.12:1.24	0.29	6.30	91.84	3761	3352
150	1	V	C^*	8	1.18:1.10:1:1.10:1.18	0.33	6.25	94.23	3627	3202
150	4	A	…	0	1:2:7:2:1	5.46	4.50	37.14	1917	1808
150	4	A	C	10	1:2.01:4.87:2.01:1	0.52	5.93	44.72	2390	2228
150	4	A	C^*	10	1:2.22:4.57:2.22:1	0.57	5.95	48.18	2156	2017
150	4	M	…	0	1:5:1:5:1	5.27	4.50	52.00	2642	2505
150	4	M	C	10	1:6.57:2.55:6.57:1	0.54	5.85	53.85	3310	3172
150	4	M	C^*	10	1:6.48:2.90:6.48:1	0.57	5.87	55.12	3225	3098
150	4	V	…	0	4:2:1:2:4	4.92	4.50	65.00	2705	2514
150	4	V	C	14	4.05:2.20:1:2.20:4.05	0.45	6.04	66.67	3115	2907
150	4	V	C^*	14	3.91:2.34:1:2.34:3.91	0.43	6.01	69.05	2954	2759

be calculated as in the following equation:

$$t_{red} = \frac{\frac{d_{\max}}{D} \times I_{bx} - \sum_{k=1}^{\frac{d_{\max}}{D}} l_{eff_{\max_k}}}{\frac{d_{\max}}{D} \times I_{bx}} \times 100\%, \quad (8)$$

where $l_{eff_{\max_k}}$ is the largest effective width among features in the kth pass.

In Fig. 12, t_{red} in the case of $I_{bx} = l + s$, $l_i \neq l_j$, and nonuniform dose distribution is provided. Similar to the case in Fig. 11, the higher the dose difference among the pixels in the feature, the larger t_{red}.

c. $I_{bx} \neq l + s$: Uniform dose distribution. When $I_{bx} \neq l + s$, $l_i = l_j$, and the dose distribution is uniform, empty cycles are not found in the steady state in the conventional writing method as illustrated in Fig. 13, where $I_{bx} > l + s$. In Fig. 13, the pixels exposed by the beams in four consecutive cycles are shown for the conventional writing method. The four cycles are repeated in the steady state as the substrate moves underneath the beams. One or more beams are always on in the steady state. Hence, there are no empty cycles to be removed by the proposed writing method. Few empty cycles may be found in the transient state, which is a small fraction of the total exposing time. Hence, t_{red} is very small in this case (Fig. 14).

In the case of $I_{bx} \neq l + s$, $l_i \neq l_j$, and uniform dose distribution, empty cycles may be observed (see Fig. 15). A random selection of the feature widths and spaces may cause the beams to be turned off together in some cycles. The simulation results for such a case are provided in Fig. 16.

d. $I_{bx} \neq l + s$: Nonuniform dose distribution. When $I_{bx} \neq l + s$ (either $l_i = l_j$ or $l_i \neq l_j$), and the dose distribution is nonuniform, empty cycles are not found in the conventional writing method in the first pass (similar to the illustration in Fig. 13) in the steady state. In the later passes, the number of pixels in the feature requiring nonzero doses, l_{eff}, gets smaller depending on the shape of dose distribution, which may lead to a few empty cycles in the conventional writing method in the steady state (similar to the illustration in Fig. 15). The smaller l_{eff} becomes in a pass, the higher the chance of finding empty cycles in that pass. Therefore, t_{red} is relatively small in this case (Figs. 17 and 18) but larger than the case when $I_{bx} \neq l + s$ and the dose distribution is uniform.

2. Varying total dose from feature to feature

For correcting the proximity effect, the features on the edges of a pattern tend to get higher doses than the features in the center. This type of variation of total dose from feature to feature increases the probability of getting empty cycles in the conventional writing method compared to the nonvarying total dose from feature to feature. This is because after giving the required doses to the features in the center in the first few passes, the later passes are used only to give the remaining doses to the features on the edges and the beams are turned off together when they fall on the features in the center. Therefore, t_{red} is larger when the total dose varies from feature to feature compared to when the total dose does not vary. Also, the higher the dose difference among the features of a pattern, the larger t_{red} since the number of passes to give doses to the features on the edges, which cause empty cycles, becomes larger.

In Figs. 19 and 20, t_{red} in the case of $I_{bx} = l + s$ and uniform dose distribution is provided for $l_i = l_j$ and $l_i \neq l_j$, respectively. The only difference between this case and the case considered in Sec. VI A 1 "$I_{bx} = l + s$: Uniform dose distribution" is the variation of total dose from feature to feature. It is observed that the trend of t_{red} with respect to pattern width is similar, but t_{red} is larger as seen in Figs. 19 and 20, compared to that in Figs. 8 and 9, respectively. Similarly, when $I_{bx} = l + s$, $l_i = l_j$, or $l_i \neq l_j$ and the dose distribution is non-uniform, t_{red} is larger as seen in Figs. 21 and 22 for varying total dose from feature to feature, compared to that in Figs. 11 and 12, respectively, for nonvarying total dose from feature to feature.

In Figs. 23 and 24, t_{red} in the case of $I_{bx} \neq l + s$ and uniform dose distribution is provided for $l_i = l_j$ and $l_i \neq l_j$, respectively. It is observed that t_{red} in Figs. 23 and 24 is significantly larger than that in Figs. 14 and 16, respectively, where the total dose does not

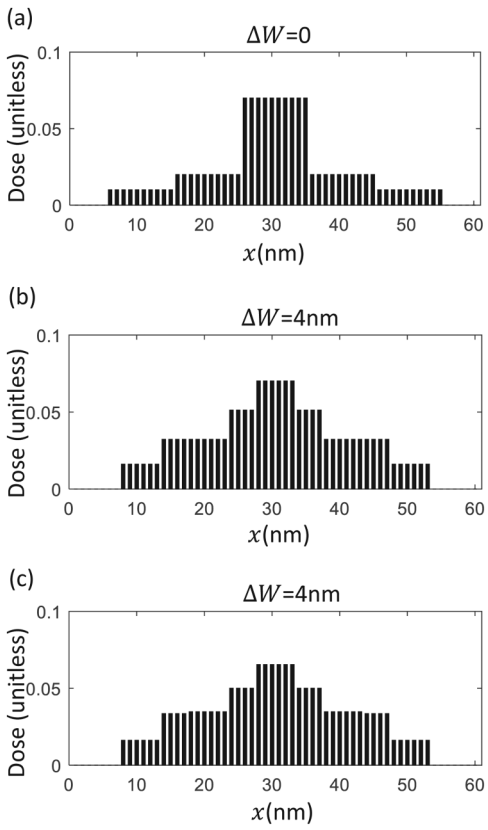

FIG. 27. A-type dose distribution obtained (a) without PEC optimization, (b) with PEC optimization not employing the method of reducing the dose difference, and (c) with PEC optimization employing the method of reducing the dose difference for the case when $l = 50$ nm and $\sigma_t = 1$ nm.

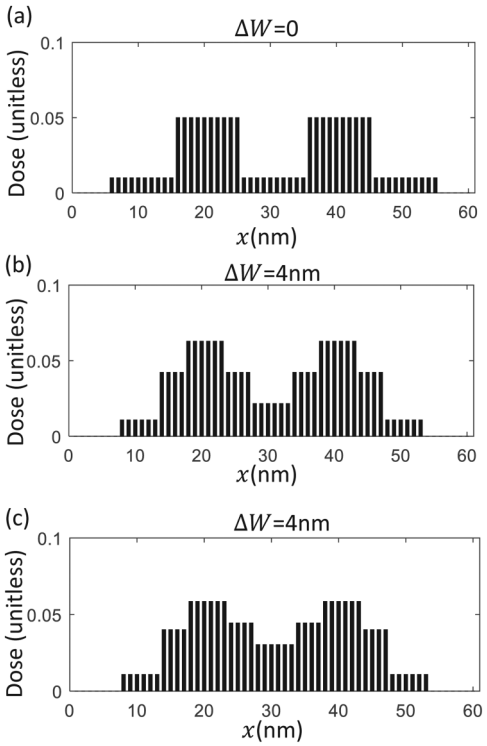

FIG. 28. M-type dose distribution obtained (a) without PEC optimization, (b) with PEC optimization not employing the method of reducing the dose difference, and (c) with PEC optimization employing the method of reducing the dose difference for the case when $l = 50$ nm and $\sigma_t = 1$ nm.

vary from feature to feature. This is because the variation of total dose from feature to feature results in empty cycles in the steady state in the conventional writing method even when $I_{bx} \neq l + s$, but empty cycles are not found in the steady state in the case of nonvarying total dose from feature to feature. Similarly, when $I_{bx} \neq l + s$, $l_i = l_j$, or $l_i \neq l_j$ and the dose distribution is nonuniform, t_{red} is substantially larger as seen in Figs. 25 and 26 than that in Figs. 17 and 18, respectively, because of the variation of total dose and a small l_{eff} in the passes for giving doses on the edges of the pattern.

B. Reduction of exposing time by reducing dose difference among the regions

In Table I, the three cases, i.e., no PEC optimization, PEC optimization without the method of reducing the dose difference (refer to Sec. IV B), and PEC optimization with the method of reducing the dose difference, are compared in terms of the CD error, total dose, beam utilization, and exposing time. To obtain a comprehensive set of results, the feature width, blurring factor of TF, and dose distribution type are varied. For calculating the exposing time, it is assumed that $I_{bx} \neq l + s$. The A-type, M-type, and V-type dose distributions obtained for each of the above-mentioned cases when $l = 50$ nm and $\sigma_t = 1$ nm are provided in Figs. 27–29, respectively. From Table I, it can be seen that, compared to the case without PEC optimization, the cases with PEC optimization achieve a significantly smaller CD error while maintaining the total dose within an acceptable limit. By comparing the optimization results with and without the method of reducing the dose difference, it is found that the increase in the CD error is marginal, but the increase in U and the reduction of exposing time are significant for both the conventional and the proposed writing methods. The beam utilization depends on the dose difference among the regions and the exposing time depends on the total dose and the maximum dose $d_{\max}$ among the regions. In the procedure to reduce the dose difference among the regions, the total dose is kept constant by lowering $d_{\max}$ with a certain amount and evenly distributing that amount to the nearby regions. The increased doses in the nearby regions compensate for the reduced $d_{\max}$ in the resist development. Hence, the increase in the CD error is not substantial, while the increase in beam utilization and the reduction of exposing time are significant. Furthermore, Table I shows the exposing time required for both the conventional writing (single-row writing) method and the proposed writing method. Hence, the reduction of exposing time by both the proposed writing method

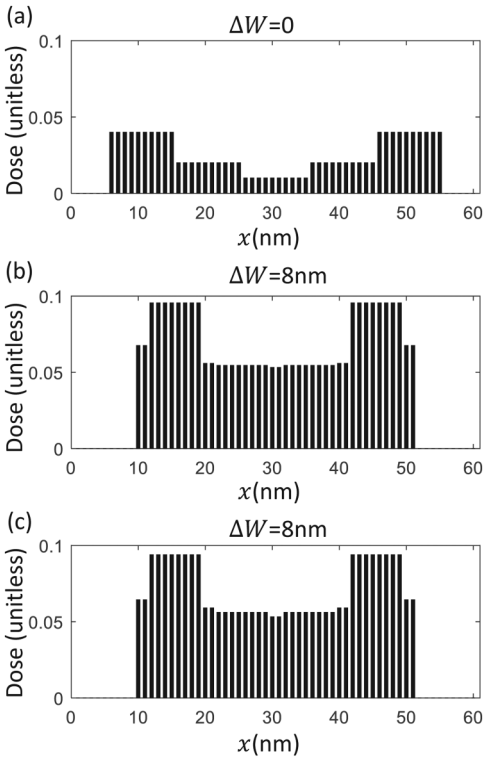

FIG. 29. V-type dose distribution obtained (a) without PEC optimization, (b) with PEC optimization not employing the method of reducing the dose difference, and (c) with PEC optimization employing the method of reducing the dose difference, for the case when $l = 50$ nm and $\sigma_t = 1$ nm.

and the lowering of dose difference among the regions in the PEC process can also be observed by comparing the exposing time of the conventional writing method when the method of reducing the dose difference is employed and that of the proposed writing method when the method is not. It is seen that even when $I_{bx} \neq l + s$, the reduction in the exposing time is significant.

VII. SUMMARY

Several writing methods were introduced previously for the massively-parallel electron-beam systems, e.g., single-row writing (SRW) and multirow writing (MRW). A straight-forward application of these methods for realizing nonuniform dose distributions including line/space patterns with a uniform dose within each line would turn off certain beams selectively in many cycles. Depending on the target dose distribution and the relationship among I_{bx}, l_i, and s_i (the beam interval, the width of the feature i in a pattern, and the space between two adjacent features i and $i+1$), sometimes all beams in a system may be turned off resulting in empty cycles. In order to enhance beam utilization and thereby reduce the exposing time, the proposed writing method removes the empty cycles in the conventional writing methods by adjusting the deflection angle of beams. From the results, it is observed that the proposed writing method can shorten the exposing time significantly, especially in the case of $I_{bx} = l + s$. In some cases with $I_{bx} \neq l + s$, the proposed writing method may not reduce the exposing time notably. In another method to reduce the exposing time, the dose difference among the regions of a feature in the optimal dose distribution for the proximity effect correction is reduced through an iterative procedure to improve beam utilization. It is demonstrated that the exposing time can be reduced substantially with a little effect on the accuracy of critical dimension. Moreover, the two proposed methods can be combined to shorten the exposing time significantly even when $I_{bx} \neq l + s$.

ACKNOWLEDGMENTS

This work was supported in part by a research grant from Samsung Electronics Co., Ltd. The authors are thankful to Hyesung Ji for his involvement in the early study on realization of spatial dose distributions on a MPES.

AUTHOR DECLARATIONS

Conflict of Interest

The authors have no conflicts to disclose.

DATA AVAILABILITY

The data that support the findings of this study are available within the article.

REFERENCES

[1]S.-Y. Lee and B. D. Cook, IEEE Trans. Semicond. Manuf. **11**, 117 (1998).
[2]S. J. Wind, P. D. Greber, and H. Rothuizen, J. Vac. Sci. Technol. B **16**, 3262 (1998).
[3]M. Osawa, K. Takahashi, M. Sato, H. Arimoto, K. Ogino, H. Hoshino, and Y. Machida, J. Vac. Sci. Technol. B **19**, 2483 (2001).
[4]S.-Y. Lee, S. C. Jeon, J. S. Kim, K. N. Kim, M. S. Hyun, J. J. Yoo, and J. W. Kim, J. Vac. Sci. Technol. B **27**, 2580 (2009).
[5]Q. Dai, S.-Y. Lee, S.-H. Lee, B.-G. Kim, and H.-K. Cho, J. Vac. Sci. Technol. B **30**, 06F307 (2012).
[6]B. J. Lin, J. Micro/Nanolith. MEMS MOEMS **11**, 033011 (2012).
[7]P. Petric, C. Bevis, A. Carrol, H. Percy, M. Zywno, K. Standiford, A. Brodie, N. Bareket, and L. Grella, J. Vac. Sci. Technol. B **27**, 161 (2009).
[8]C. Klein and E. Platzgummer, Proc. SPIE **9985**, 998505 (2016).
[9]C. Klein, H. Loeschner, and E. Platzgummer, J. Micro/Nanolith. MEMS MOEMS **11**, 031402 (2012).
[10]H. Matsumoto, H. Inoue, H. Yamashita, T. Tamura, and K. Ohtoshi, J. Micro/Nanolith. MEMS MOEMS **17**, 031205 (2018).
[11]A. Fay *et al.*, Proc. SPIE, **9777**, 977714 (2016).
[12]H. Fragner and E. Platzgummer, U.S. patent 7777201 B2 (17 August 2010).
[13]S.-Y. Lee, B.-S. Ahn, J. Choi, S.-B. Kim, and C.-U. Jeon, J. Vac. Sci. Technol. B **37**, 061602 (2019).
[14]M. N. Hasan, S.-Y. Lee, B.-S. Ahn, J. Choi, S.-B. Kim, and C.-U. Jeon, J. Vac. Sci. Technol. B **37**, 061609 (2020).
[15]M. N. Hasan, S.-Y. Lee, B.-S. Ahn, J. Choi, and J.-S. Park, J. Vac. Sci. Technol. B **38**, 062603 (2020).
[16]D. Drouin, A. R. Couture, D. Joly, X. Tastet, V. Aimez, and R. Gauvin, Scanning **29**, 92 (2007).
[17]Q. Dai, R. Guo, S.-Y. Lee, J. Choi, S.-H. Lee, I.-K. Shin, and C.-U. Jeon, Microelectron. Eng. **127**, 86 (2014).